BIOSCIENCES BIOTECHNOLOGY RESEARCH ASIA, March 2026. Vol. **23**(1), p. 254-263

Silver Nanorods Induced Cytotoxicity, Oxidative Stress and Inflammation in Human A549 Lung Cells

Zareena Begum Shaik[1] and Harikiran Lingabathula[2]*

[1]Department of Pharmaceutics, Princeton College of Pharmacy, Telangana, India.
[2]Department of Pharmacology and Toxicology, Princeton College of Pharmacy, Telangana, India.

http://dx.doi.org/10.13005/bbra/3495

(Received: 08 December 2025; accepted: 10 March 2026)

Silver nanorods are widely employed in a variety of commercial, industrial, and biological applications. Although silver nanorods have several uses, nothing is known about their toxicity. This research aimed to evaluate the laboratory-based harmful effects of silver nanorods measuring 10 nm and 25 nm following exposure to human lung A549 cell lines. The cell viability was tested using tetrazolium assay and lactate dehydrogenase leakage assays . The oxidative stress induction markers such as, lipid peroxidation, glutathione levels and caspase-3 levels were estimated. And the inflammatory mediator interleukin-8 was estimated using biochemical assay kit. Cells exposed to silver nanorods displayed reduced cell viability and increased lactate dehydrogenase leakage, indicating cytotoxicity. Additionally, exposure to silver nanorods causes elevated levels of the inflammatory mediator interleukin-8, decreased levels of glutathione, and increased levels of lipid peroxidation and caspase-3, which indicate oxidative stress. When compared to 25 nm silver nanorods and quartz, a recognized toxicant, the 10 nm silver nanorods showed higher toxicity towards all metabolic parameters. Finally, our results suggesting that the toxicity of silver nanorods was dependent on their concentration and size.

Keywords: Caspase-3; Interleukin-8; In vitro toxicity; Nanorods; Silver nanoparticles.

Due to their special mechanical, optical, physicochemical, and functionalization characteristics, silver nanoparticles (SNP) have enormous potential for future applications.[1] SNP possess an increased ability to defend against a wide range of microbes and fungi compared to their microsized particles.[2] The SNP are also used in medical devices, biosensors, refrigerators, textiles, cosmetics and also in various other consumer applications.[3]

SNP can be available in different morphology and nanorod is one of them with the majority of research focused because of their ample range of applications over spherical nanoparticles. The food industry, cosmetics, sunscreens, diagnostic tracers, medical devices, biosensing, imaging, and antimicrobial applications are the main uses for silver nanorods (SNR).[4,5] Additionally, the SNR were employed to detect residues of chloropropanol and as a high brightness photocathode material.[6,7]

Despite the widespread use of SNP, exposure to these nanoparticles also significantly increased. A recent investigation explored the detrimental impacts of SNP on various cell types, including human lung cells (A549), fibroblasts (NIH-3T3), rat adrenal pheochromocytoma

*Corresponding author E-mail: harikiran.pharma@gmail.com

cells (PC-12), and human liver cell lines (HEP G2).[8] The results have shown that SNP were considerably more toxic towards all cell lines tested than the silver ions, suggest that the toxicity of SNP. After exposure to different types of nanoparticles, oxidative stress and the production of reactive oxygen species (ROS) have been shown to serve as significant elements in the cellular defense mechanism.[9-11] Recent studies on SNP have revealed the toxicities they cause in a variety of human cell lines and animals.[12–14] Their characteristics, such as the size and shape of SNP, significantly influenced the degree of toxicity.[15,16]

However, several recent investigations have examined the toxic effects of SNR on cells using various human cell line models and recorded the cellular toxicity that SNR induced across different cell types.[17] This study aimed to evaluate the potential cellular toxicity, oxidative damage, and inflammatory responses of rod-shaped, polyethylene glycol (PEG) functionalized 10 nm SNR and 25 nm SNR in human lung epithelial (A549) cells and to compare these findings with control groups and quartz (QTZ), an established toxic reference material.

MATERIALS AND METHODS

Chemicals

The 10 nm SNR (indicated as SNR 10) and 25 nm SNR (indicated as SNR 25) were supplied by Sigma-Aldrich, Bangalore. As per the manufacturer's specifications, the nanoparticles exhibited rod-shaped morphology with defined dimensions. SNR 10 had an average diameter of 10 nm and length of 31–51 nm, while SNR 25 had an average diameter of 25 nm and length of 50–70 nm, corresponding to defined length-to-diameter aspect ratios. Manufacturer-provided physicochemical characterization data were used as reference specifications in this study. No additional TEM/SEM analysis was performed in the present study; therefore, particle dimensions are reported according to supplier specifications. Quartz particles (58–68 µm) were purchased from Berkely Springs, USA. Cell culture grade materials including Dulbecco's modified eagle's medium (DMEM), 1% streptomycin-penicillin antibiotic solution, fetal bovine serum (FBS), 1% L-glutamine, PEG, trypsin-EDTA (0.25%) and phosphate buffer saline (PBS) were obtained from Himedia, Mumbai. Dimethylsulphoxide (DMSO) was acquired from Merck India Ltd. in India. The 3-(4,5-dimethyl thiazol-2-yl)-2,5-diphenyl tetrazolium bromide (MTT) was sourced from Sigma-Aldrich, Bangalore. Ray Biotech, based in New Delhi, India, supplied all biochemical assay kits used in this study.

Cell line and treatment

Human lung A549 cells were obtained from the NCCS located in Pune, India. The lung cells employed were from passages 12 through 15. Cell cultivation was performed using DMEM medium containing 10% FBS, 1% L-glutamine, and 1% penicillin-streptomycin antibiotic mixture. A total of 250,000 cells were placed in each flask with 10 mL total volume. Following confluence achievement, cells underwent trypsinization using trypsin-EDTA solution and were subsequently plated in 96-well plates at $1.0x10^4$ cells per 0.1 mL. Cell cultures were maintained in a CO_2 incubator (WTC Binder, Germany) at 37^0C with 5% CO_2 atmosphere.[18]

Test SNR suspensions were prepared at a density of 0.986g/mL at 25^0C employing PBS as the dissolution medium and PEG (<1%) for stabilization purposes. For parameter evaluation, newly prepared test SNR and QTZ concentrations ranging from 10-50 µg/mL were prepared in serum-free culture medium, alongside control samples containing PBS with 1% PEG.[18] The experimental conditions, including incubation duration (24 h exposure) and *in vitro* cell-based cytotoxicity assessment are consistent with the present study. Although the earlier study employed a different cancer cell model, both systems represent epithelial-origin human cancer cells cultured under standard conditions (37°C, 5 % CO, , serum-supplemented medium). Such methodological similarity supports the translational applicability of the previously established concentration window to A549 lung adenocarcinoma cells.[18]

Cell viability test

The tetrazolium assay technique was employed to assess how test SNR affected cell viability and growth.[19] Metabolically active cells containing dehydrogenase enzymes reduced the yellow tetrazolium salt through their mitochondria, producing the reducing equivalents NADH and NADPH. The resulting formazan, which

exhibited limited water solubility and appeared as purple crystals, was dissolved using DMSO. This facilitated straightforward measurement of product formation. The intensity of the product's color, measured at 562 nm, showed a direct relationship with the quantity of viable cells present in the culture. For this assay, cells were planted in 96-well plates (Tarsons, Mumbai, India), and SNR suspensions (100 µL, performed in triplicate) in medium were introduced.[18]

After a 48-hour incubation at 37^0C in a 5% CO_2 incubator, 20µ L of MTT solution (5 mg/mL) was introduced to each microtiter plate well. The microtiter plate was wrapped with aluminum foil to protect the dye from oxidation, DMSO (80 µL) was dispensed into each well, and the plate underwent another two-hour incubation period. The plate was placed on a rotary shaker (Remi equipment, India) for two hours to achieve proper mixing. Absorbance readings were subsequently recorded using an ELISA reader (Anthos 2010, Germany).[18] Cell viability was calculated by comparing the experimental absorbance values against the solvent control.

Cell extract preparation

A549 human lung cells were planted in 100 µL of culture media at a concentration of $1.0x10^4$ cells per each well in a sterilized 96-well plate. In triplicate, 100 µL of test SNR suspensions at progressively higher concentrations were applied to each well. For 48 hours, the microtiter plate was kept at 37^0C in an incubator with 5% CO_2. After being extracted, the supernatants were put into a brand-new microtiter plate. The manufacturer's instructions were followed while using the cell supernatants for various biochemical tests.

Biochemical assays

Lactate dehydrogenase (LDH) is a soluble cytosolic enzyme that contains zinc. Its leakage into culture media can be used to quantify cytotoxicity by indicating the integrity of the cell membrane.[20] Oxidation-reduction homeostasis in cells is maintained by glutathione (GSH), which is chemically a tripeptide (ã-glutamylcysteinylglycine). Reduced GSH levels signify the onset of oxidative stress.[21] The amount of malondialdehyde, a naturally occurring as a result of peroxidation of lipids, was quantified by measuring thiobarbituric acid reactive substances (TBARS), a common technique for estimating lipid peroxidation.[22]

Caspases constitute a group within the protease family and are classified as aspartate-specific cysteinyl proteases. A biomarker for estimating apoptosis and comprehending the mechanisms underlying apoptosis induction is the activation of caspase-3.[23] Many cell types secrete Interleukin-8, a protein that attracts neutrophils and indicates the presence of inflammation, is released by numerous types of cells.[24] Every metric was calculated and shown as a percentage of control.

Statistical analysis

Using Graph Pad Prism 9, the inhibitory concentration 50 (indicating as IC50) was determined when at least two viability values fell below 50% of the control condition.[18] Mean±S.D. was used to express the data (n=4). All biochemical assays were subjected to statistical analysis using ANOVA and Bonferroni posttests. The statistical significance was shown by $^a p<0.05$, $^b p<0.01$, $^c p<0.001$ compared to QTZ particles and $^\# p<0.01$, $^* p<0.001$ versus control (PBS+1% PEG).

RESULTS

At dosages of 10–50 µg/mL, the results demonstrated a significant decrease in cell viability for QTZ, 10 nm SNR and 25 nm SNR in comparison to the control (Figure 1). Additionally, at 30 µg/mL and 50 µg/mL doses, 10nm SNR significantly reduced cell viability in comparison to QTZ with a P value less than 0.001. The IC50 values for SNR at 10nm and 25nm were determined to be 18.23 µg/mL and 23.82 µg/mL, respectively. Compared to control cells, the lung cells exposed to both SNR significantly leaked LDH into medium at concentrations of 30 µg/mL and 50 µg/mL (Figure 2). In comparison to QTZ-treated cells, the 10 nm SNR at 50 µg/mL concentration significantly increased the LDH leakage with a P value less than 0.001.

The levels of GSH were markedly decreased in A549 cells exposed to both types of SNR at doses of 30µg/mL and 50µg/mL when compared to control cells (Figure 3). The 10nm SNR at 10µg/mL concentration also demonstrated a notable ($p<0.01$) reduction in GSH levels relative to control cells. When lung cells were exposed to

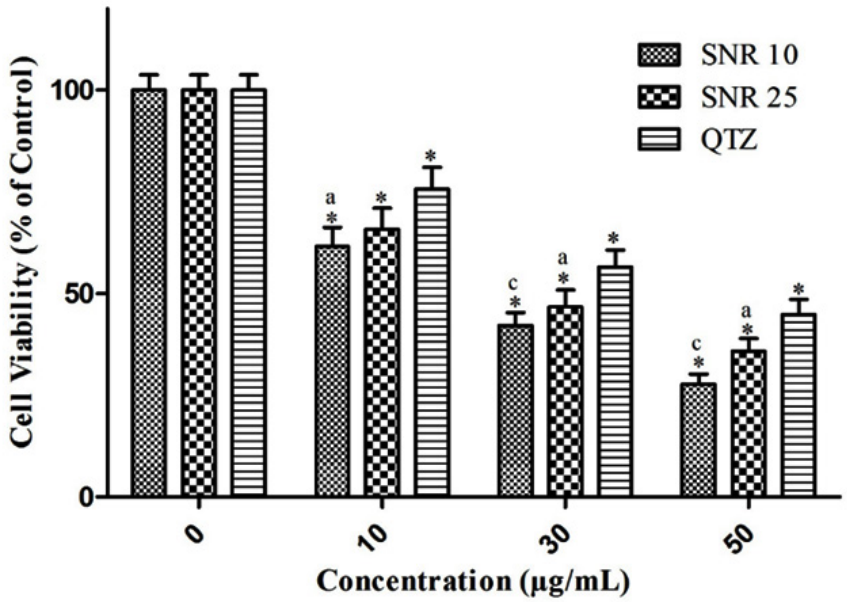

Fig. 1. Cell viability (% of control) in human lung (A549) cells following exposure of SNR. Mean±S.D. was used to express the data (n=4 independent biological replicates). Significance was shown by [a]p<0.05, [b]p<0.01, [c]p<0.001 compared to QTZ and [#]p<0.01, *p<0.001 compared to vehicle control

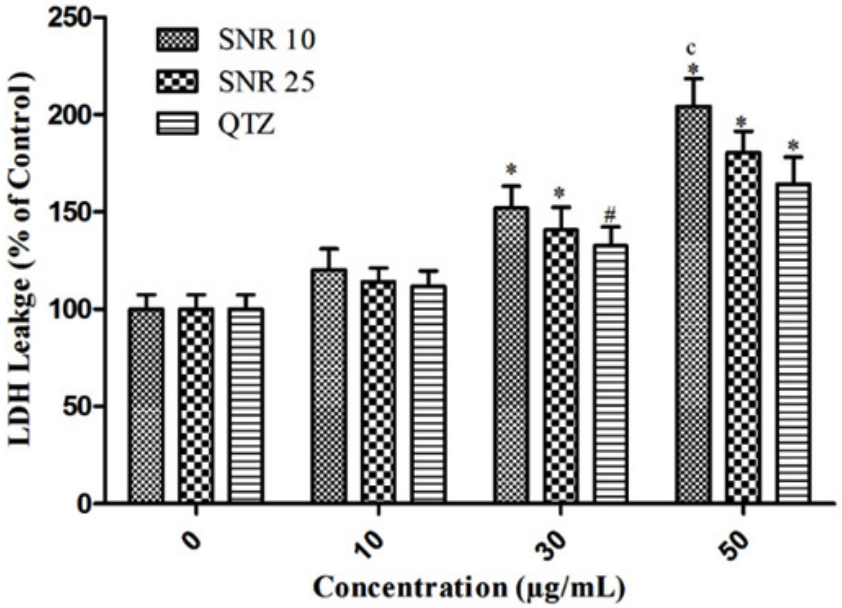

Fig. 2. Lactate dehydrogenase leakage (% of control) in human lung (A549) cells following exposure of SNR. Mean±S.D. was used to express the data (n=4 independent biological replicates). Significance was shown by [a]p<0.05, [b]p<0.01, [c]p<0.001 compared to QTZ and [#]p<0.01, *p<0.001 compared to vehicle control

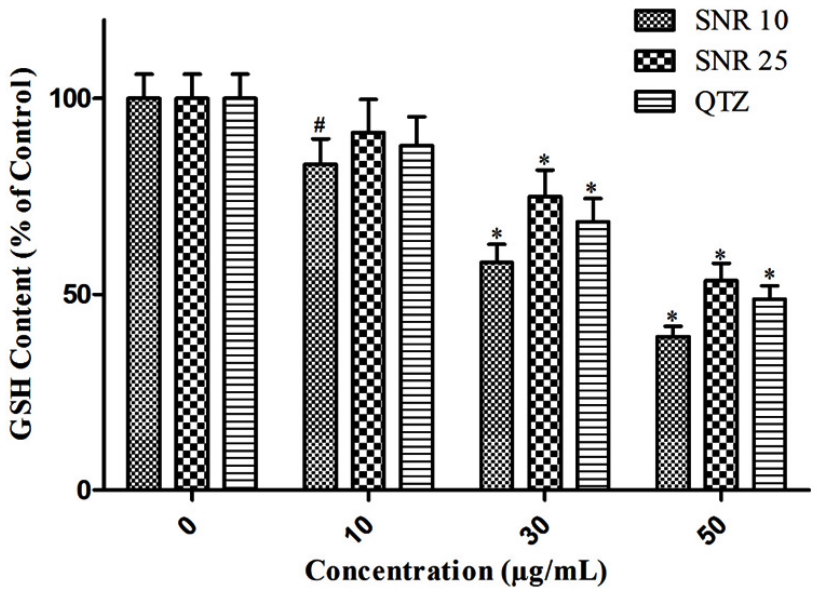

Fig. 3. Glutathione content (% of control) in human lung (A549) cells following exposure of SNR. Mean±S.D. was used to express the data (n=4 independent biological replicates). Significance was shown by [a]p<0.05, [b]p<0.01, [c]p<0.001 compared to QTZ and [#]p<0.01, *p<0.001 compared to vehicle control

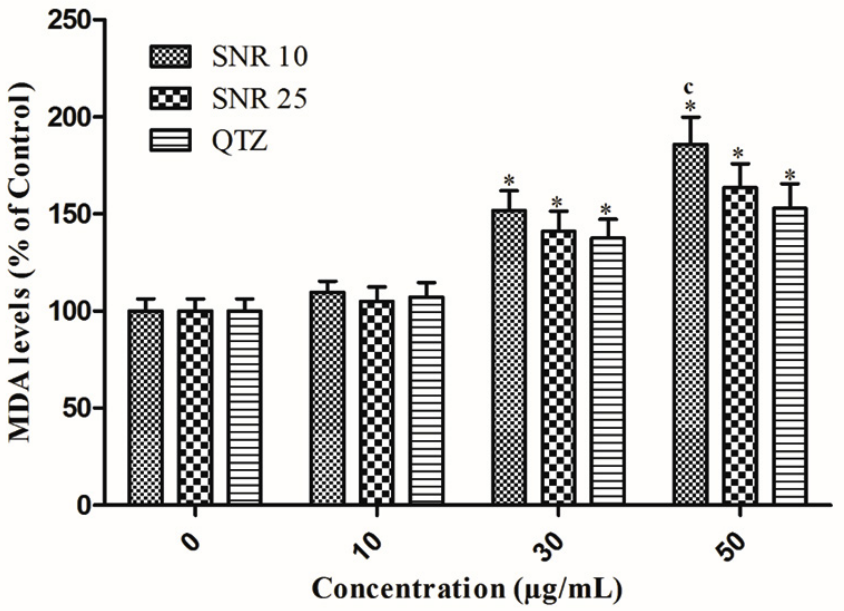

Fig. 4. Malondialdehyde levels (% of control) in human lung (A549) cells following exposure of SNR. Mean±S.D. was used to express the data (n=4 independent biological replicates). Significance was shown by [a]p<0.05, [b]p<0.01, [c]p<0.001 compared to QTZ and [#]p<0.01, *p<0.001 compared to vehicle control

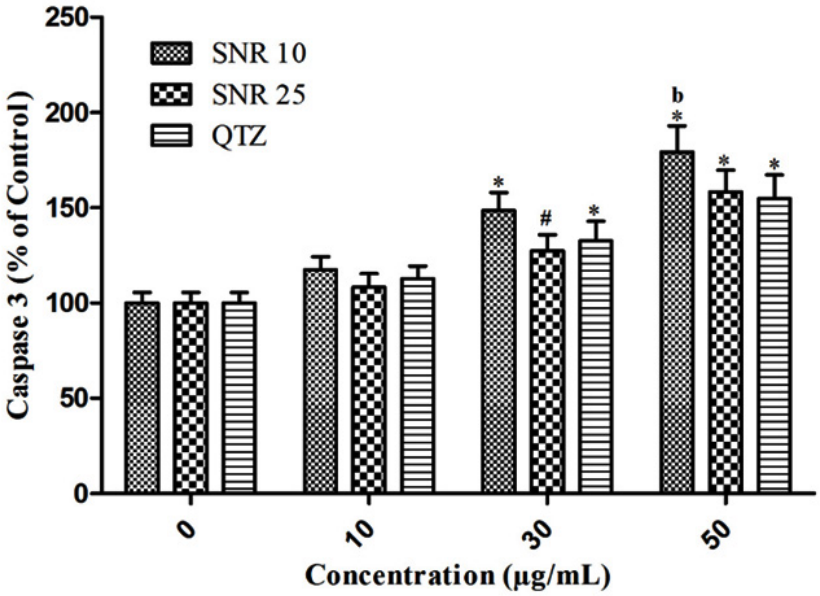

Fig. 5. Caspase-3 levels (% of control) in human lung (A549) cells following exposure of SNR. Mean±S.D. was used to express the data (n=4 independent biological replicates). Significance was shown by [a]p<0.05, [b]p<0.01, [c]p<0.001 compared to QTZ and [#]p<0.01, *p<0.001 compared to vehicle control

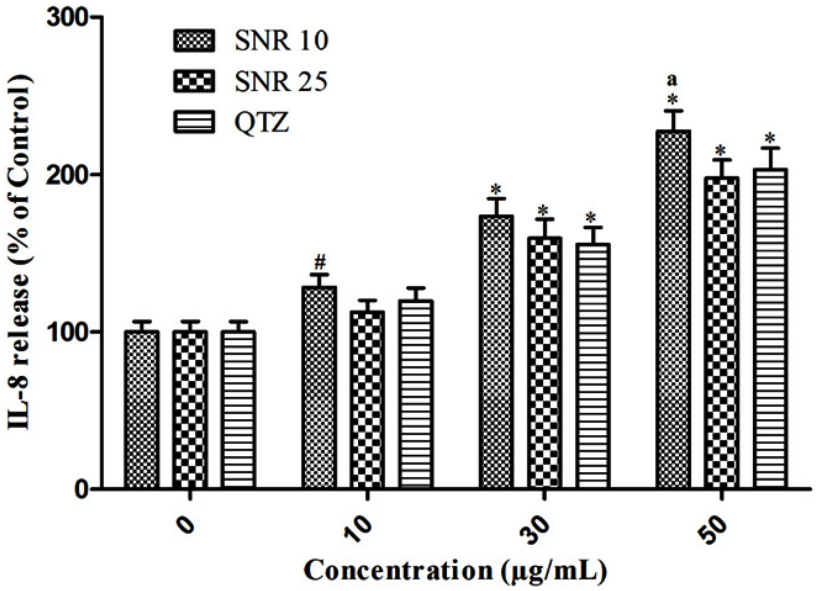

Fig. 6. Interleukin-8 release (% of control) in human lung (A549) cells following exposure of SNR. Mean±S.D. was used to express the data (n=4 independent biological replicates). Significance was shown by [a]p<0.05, [b]p<0.01, [c]p<0.001 compared to QTZ and [#]p<0.01, *p<0.001 compared to vehicle control

both SNR types at 30µg/mL and 50µg/mL doses, MDA concentrations were substantially elevated compared to control cells, while the 10nm SNR at 50µg/mL produced a pronounced increase in MDA levels ($p<0.001$) when compared to QTZ treated cells (Figure 4).

The results demonstrated that both 10nm SNR and 25nm SNR increased caspase-3 expression when administered at concentrations of 30µg/mL and 50µg/mL relative to control groups. Additionally, 10nm SNR at the 50µg/mL dose produced a statistically significant ($p<0.01$) increase in caspase-3 expression when compared to QTZ treated cells (Figure 5). A549 lung cells exhibited markedly elevated IL-8 levels relative to control samples when exposed to both SNR particle sizes at the 30µg/mL and 50µg/mL treatment concentrations (Figure 6). Additionally, compared to cells treated with QTZ, 10nm SNR at a concentration of 50µg/mL showed considerably higher levels of IL-8 ($p<0.001$).

DISCUSSION

Using several biochemical tests in comparison to control and QTZ, the current work examined the *in vitro* cytotoxicity, development of oxidative stress and stimulation of inflammation of two sizes (10nm and 25nm) of SNR against the human lung (A549) epithelial cells. Human A549 lung cells were used in the MTT experiment to assess the impact of SNR on cell viability, and both SNR showed increased cytotoxicity against lung cells. Two sizes of SNR had IC50 values that were lower than the QTZ, indicating that SNR were more cytotoxic. The LDH leakage assay was used to assess the cell membrane injury caused by the investigated SNR. The cytotoxicity of SNR was demonstrated in our work by the increased amounts of LDH that were released into media containing both sizes of SNR as a function of concentration. Rat brain endothelial cells were used to test the in vitro toxicity of spherical SNP. The results showed that a 24-hour exposure significantly reduced dye uptake using the neutral red assay, a marker of cytotoxicity.[13]

Treatment of A549 cells with 10nm SNR and 25nm SNR may have caused oxidative stress induction and ROS generation through GSH depletion and elevated MDA levels indicating enhanced lipid peroxidation, resulting in lung cell functional impairment. Lung cells exposed to both sizes of SNR had higher amounts of caspase-3, which caused cytotoxicity. SNR exposure in A549 cells showed a higher capacity to reduce GSH content, elevation in lipid peroxidation, and levels of caspase-3 were boosted, all of which cause oxidative stress and cytotoxicity.

It has been demonstrated that SNP result in cellular toxicity in many cell types through reduced GSH levels, elevated caspase-3 levels, increased lipid peroxidation, and ROS production as a result of oxidative stress induction, which ultimately triggers the start of apoptosis.[25-27] After being treated with various nanoparticles, higher levels of the cytokine IL-8 were found in several cell types, which is an indication of inflammation.[28,29] After A549 cells were treated with 10nm SNR and 25nm SNR, elevated expression of IL-8, an indication of inflammation, were observed. The results of our investigation were corroborated by recent research that showed the inflammatory response caused by gold and silver nanoparticles in human A549 cells and human mesenchymal stem cells in the form of markedly elevated levels of IL-8 release.[30,31]

In comparison to control and QTZ-treated lung cells, our analysis showed that the 10nm SNR dramatically decreased cell viability, GSH content, elevated LDH leakage, enhanced lipid peroxidation, increased caspase-3 levels and raised IL-8 levels. The greater toxicity of 10nm SNR to lung cells is demonstrated by the fact that the 25nm SNR also had comparable impacts on the evaluated biochemical parameters, although not as much as the 10nm SNR.

Numerous research on various nano material sizes have recently been carried out, and the results indicate that smaller nano materials have the potential to cause more cytotoxicity, oxidative stress, ROS production, and inflammation than larger nano materials.[18,32] Studies that looked at the toxicity of SNP of various sizes found that the smaller SNP were more harmful than the bigger ones.[33–35] These investigations indicate that 10nm SNR are more cytotoxic than 25nm SNR.

A limitation of the present study is that nanoparticle dispersion stability was not characterized in complete cell culture medium using DLS or zeta potential analysis. Although suspensions were ultrasonicated prior to dosing,

aggregation during the 48-h incubation period cannot be ruled out due to protein corona formation and medium ionic strength. Consequently, the effective hydrodynamic size of the nominal 10 nm SNRs at the cellular interface may have been larger than the primary particle size, and thus conclusions regarding strict size-dependent toxicity should be interpreted cautiously.

CONCLUSION

Human lung epithelial cells exposed to 10nm SNR and 25nm SNR *in vitro* demonstrated cytotoxicity using the microculture tetrazolium test and cell membrane injury by increased leakage of LDH enzyme. Increased oxidative stress has been demonstrated by SNR exposure by decreased levels of GSH, increased peroxidation of lipids, higher levels of caspace-3, and elevated levels of IL-8, which indicate the production of inflammation in A549 cells. Concentration-size-dependent toxicity is revealed by treating SNR with lung cells *in vitro*. To clarify the molecular pathways of SNR toxicity *in vivo*, more research is necessary.

ACKNOWLEDGEMENTS

The authors are very grateful to Princeton College of Pharmacy for providing necessary facilities to carry out the project.

Funding Source

The author(s) received no financial support for the research, authorship, and/or publication of this article.

Conflict of Interest

The authors report no conflicts of interest.

Data Availability Statement

This statement does not apply to this article.

Ethics Statement

This research did not involve human participants, animal subjects, or any material that requires ethical approval.

Informed Consent Statement

This study did not involve human participants, and therefore, informed consent was not required. Clinical Trial.

Clinical Trial Registration

This research does not involve any clinical trials.

Permission to reproduce material from other sources

Not Applicable

Author Contributions

Zareena Begum Shaik: Data Collection, Analysis and Writing; Harikiran Lingabathula: Conceptualization, Methodology, Supervision, Review and Editing

REFERENCES

1. Sang HL, Bong HJ. Silver nanoparticles: synthesis and applications for nanomedicine. *Int J Mol Sci*. 2019;20:865. doi:10.3390/ijms20040865
2. Iris XY, Jing Z, Irene SZ, et al. The antibacterial mechanism of silver nanoparticles and its application in dentistry. *Int J Nanomedicine.* 2020;15:2555-2562. doi:10.2147/IJN.S246764
3. Marin S, Vlasceanu GM, Tiplea RE, et al. Applications and toxicity of silver nanoparticles: a recent review. *Curr Top Med Chem*. 2015;15:1596-1604. doi:10.2174/1568026615666150413153618
4. Li X, Yi YW, Jie H, et al. Silver nanoparticles: synthesis, medical applications, and biosafety. *Theranostics.* 2020;10:8996-9031. doi:10.7150/thno.45413
5. Prateek M, Swati J, Suman R, et al. Pharmaceutical aspects of silver nanoparticles. *Artif Cells Nanomed Biotechnol.* 2018;46(sup1):S115-S116. doi:10.1080/21691401.2018.1521239
6. Li S, Zhi GY, Wen BG, et al. Silver nanorod array electrodes and their application for detection of low concentration chloropropanol in aqueous media. *Appl Mech Mater.* 2015;697:136-139. doi:10.4028/www.scientific.net/AMM.697.136
7. Subramanian V, Manjula IN, Alan GJ, et al. Silver nanorod arrays for photocathode applications. *Appl Phys Lett.* 2013;103:161112. doi:10.1063/1.4825126
8. Sambale F, Wagner S, Stahl F, et al. Investigations of the toxic effect of silver nanoparticles on mammalian cell lines. *J Nanomater.* 2015;2015:136765. doi:10.1155/2015/136765
9. Alexandra J, Dieter GW, Ludwig J, et al. Oxidative stress-induced cytotoxic and genotoxic effects of nano-sized titanium dioxide particles in human HaCaT keratinocytes. *Toxicology.* 2012;296:27-36. doi:10.1016/j.tox.2012.02.001
10. Khanna P, Ong C, Bay BH, et al. Nanotoxicity: an interplay of oxidative stress, inflammation and cell death. *Nanomaterials.* 2015;5:1163-1180. doi:10.3390/nano5031163
11. Mohamed BM, Verma NK, Prina-Mello A,

et al. Activation of stress-related signalling pathway in human cells upon SiO, nanoparticles exposure as an early indicator of cytotoxicity. *J Nanobiotechnol.* 2011;9:29. doi:10.1186/1477-3155-9-29

12. Jennifer M, Jacek Z, Anna L, et al. Prolonged effects of silver nanoparticles on p53/p21 pathway-mediated proliferation, DNA damage response, and methylation parameters in HT22 hippocampal neuronal cells. *Mol Neurobiol.* 2017;54:1285-1300. doi:10.1007/s12035-016-9731-4
13. Susann G, Lars E, Tore S, et al. Silver nanoparticle-induced cytotoxicity in rat brain endothelial cell culture. *Toxicol In Vitro.* 2013;27:305-313. doi:10.1016/j.tiv.2012.10.006
14. Xiaomei L, Kristin S, Laetitia B, et al. Silver nanoparticle toxicity and association with the alga *Euglena gracilis*. *Environ Sci Nano.* 2015;2:594-602. doi:10.1039/C5EN00173A
15. Lankveld DP, Oomen AG, Krystek P, et al. The kinetics of the tissue distribution of silver nanoparticles of different sizes. *Biomaterials.* 2010;31:8350-8361. doi:10.1016/j.biomaterials.2010.07.045
16. Rothen RB, Brown DM, Piallier-Boyles M, et al. Relating the physicochemical characteristics and dispersion of multiwalled carbon nanotubes to oxidative reactivity and inflammation. *Nanotoxicology.* 2010;4:331-342. doi:10.3109/17435390.2010.496468
17. Favi PM, Valencia MM, Elliott PR, et al. Shape and surface chemistry effects on the cytotoxicity and cellular uptake of metallic nanorods and nanospheres. *J Biomed Mater Res A.* 2015;103:3940-3955. doi:10.1002/jbm.a.35505
18. Harikiran L, Narsimhareddy Y. Cytotoxicity, oxidative stress, and inflammation in human Hep G2 liver epithelial cells following exposure to gold nanorods. *Toxicol Mech Methods.* 2016;26(5):340-347. doi:10.1080/15376516.2016.1188242.
19. Jun SL, Won-Kyo J, Myung HJ, et al. Sanguinarine induces apoptosis of HT-29 human colon cancer cells via regulation of Bax/Bcl-2 ratio and caspase-9 pathway. *Int J Toxicol.* 2012;31:70-77. doi:10.1177/1091581811433314
20. Haslam G, Wyatt D, Kitos PA. Estimating the number of viable animal cells in multi-well cultures based on their lactate dehydrogenase activities. *Cytotechnology.* 2000;32(1):63-75. doi:10.1023/A:1008121125755. PMC
21. Anreddy RNR, Yellu NR, Devarakonda RK, et al. Multi-wall carbon nanotubes induce oxidative stress and cytotoxicity in human embryonic kidney (HEK 293) cells. *Toxicology.* 2010;272:11-16. doi:10.1016/j.tox.2010.03.017. PMC
22. Ohkawa H, Ohishi N, Yagi K. Assay for lipid peroxides in animal tissues by thiobarbituric acid reaction. *Anal Biochem.* 1979;95:351-358. doi:10.1016/0003-2697(79)90126-3.
23. Chen HW, Su SF, Chien CT, et al. Titanium dioxide nanoparticles induce emphysema-like lung injury in mice. *FASEB J.* 2006;20:2393-2395. doi:10.1096/fj.06-6155fje.
24. Baggiolini M, Walz A, Kunkel SL. Neutrophil-activating peptide-1/interleukin-8, a novel cytokine that activates neutrophils. *J Clin Invest.* 1989;84(4):1045-1049. doi:10.1172/JCI114267.
25. Alicia A, Ana IH, Diego M, et al. Cytotoxicity and ROS production of manufactured silver nanoparticles of different sizes in hepatoma and leukemia cells. *J Appl Toxicol.* 2014;34(5):413-423. doi:10.1002/jat.2985.
26. Porntipa C, Somsong L, Sittiruk R, et al. Silver nanoparticles induce toxicity in A549 cells via ROS-dependent and ROS-independent pathways. *Toxicol In Vitro.* 2013;27(2):330-338. doi:10.1016/j.tiv.2012.12.010.
27. Ying T, Yafeng S, Libin H, et al. In vitro cytotoxicity of gold nanorods in A549 cells. *Environ Toxicol Pharmacol.* 2015;39:871-878. doi:10.1016/j.etap.2015.01.017.
28. Brown DM, Dickson C, Duncan P, et al. Interaction between nanoparticles and cytokine proteins: impact on protein and particle functionality. *Nanotechnology.* 2010;21(21):215104. doi:10.1088/0957-4484/21/21/215104.
29. Samberg ME, Oldenburg SJ, Monteiro-Riviere NA. Evaluation of silver nanoparticle toxicity in skin in vivo and keratinocytes in vitro. *Environ Health Perspect.* 2010;118(3):407-413. doi:10.1289/ehp.0901392.
30. George DB, Amy A, Marlene B, et al. Cytotoxicity and inflammation in human alveolar epithelial cells following exposure to occupational levels of gold and silver nanoparticles. *J Nanopart Res.* 2012;14:1212-1221. doi:10.1007/s11051-012-0960-y.
31. Hackenberg S, Scherzed A, Kessler M, et al. Silver nanoparticles: evaluation of DNA damage, toxicity and functional impairment in human mesenchymal stem cells. *Toxicol Lett.* 2011;201(1):27-33. doi:10.1016/j.toxlet.2010.11.016.
32. Vijaykumar S, Ganesan S. Size-dependent in vitro cytotoxicity assay of gold nanoparticles. *Toxicol Environ Chem.* 2013;95(6):277-287. doi:10.1080/02772248.2013.813056.
33. Harikiran L, Narsimhareddy Y. Extra-pulmonary toxicity assessment of gold and silver nanorods

following intratracheal instillation in rats. *Drug Res (Stuttg)*. 2017;67(12):606-612. doi:10.1055/s-0043-117997.

34. Haase A, Mantion A, Graf P, et al. A novel type of silver nanoparticles and their advantages in toxicity testing in cell culture systems. *Arch Toxicol.* 2012;86(7):1089-1098. doi:10.1007/s00204-012-0843-8.

35. Van der Zande M, de Jong WH, Klaessens M, et al. The effect of particle size on the cytotoxicity, inflammation, developmental toxicity, and genotoxicity of silver nanoparticles. *Biomaterials*. 2011;32(36):9810-9817. doi:10.1016/j.biomaterials.2011.08.070.